

ENCLOSURE 5

AP1000 RCP-06-009-NP

“Structural Analysis Summary for the Reactor Coolant Pump High Inertia Flywheel”

(Non-Proprietary)

October 19, 2006



EMD

Curtiss-Wright Electro-Mechanical Corporation
Electro-Mechanical Division
Cheswick, PA 15024

Structural Analysis Summary
for the AP1000 Reactor Coolant Pump
High Inertia Flywheel

October 19, 2006

AP1000RCP-06-009-NP

TABLE OF CONTENTS

	Page
LIST OF TABLES.....	iii
LIST OF FIGURES.....	iv
EXECUTIVE SUMMARY	v
1.0 INTRODUCTION.....	1-1
2.0 SUMMARY OF RESULTS	2-1
3.0 DESCRIPTION OF COMPONENTS.....	3-1
4.0 DESIGN REQUIREMENTS	4-1
4.1 LOADING CONDITIONS	4-1
4.2 CRITERIA	4-2
4.2.1 American Society of Mechanical Engineers Code.....	4-2
4.2.2 Regulatory Guide 1.14	4-2
4.2.3 Standard Review Plan	4-3
5.0 ANALYTICAL METHODS AND RESULTS.....	5-1
5.1 FLYWHEEL CALCULATIONS.....	5-1
5.1.1 Analytical Model.....	5-2
5.1.2 Concentric Ring Model Geometry and Shrink-Fit.....	5-5
5.1.3 Outer Retainer Cylinder Rotational Primary Stresses	5-5
5.1.4 Concentric Ring Elastic Hoop Stresses	5-8
5.1.5 Flywheel Enclosure Welds.....	5-9
5.1.6 Fracture Mechanics of Outer Retainer Cylinder	5-9
5.2 MISSILE PENETRATION	5-10
5.2.1 Assumptions.....	5-10
5.2.2 Energy Analysis	5-11
5.2.3 Missile Containment Analysis Results	5-12
5.2.4 Conclusion	5-12
6.0 REFERENCES.....	6-1

LIST OF TABLES

Table 5-1	Mechanical Properties	5-3
Table 5-2	AP1000 Motor Cavity Flywheel Hoop Stresses	5-8
Table 5-3	Pump Containment Thicknesses Analyzed in Missile Analysis	5-11
Table 5-4	Pressure Boundary Capacity for Missile Containment	5-12

LIST OF FIGURES

Figure 3-1	AP1000 Canned-Motor Reactor Coolant Pump.....	3-2
Figure 5-1	Flywheel Assembly Dimensions	5-4

EXECUTIVE SUMMARY

This report summarizes the evaluation of the high inertia flywheel assembly for the AP1000 reactor coolant pump. The AP1000 reactor coolant pump is a single-stage, hermetically sealed, high-inertia, centrifugal canned-motor pump. The pump motor and all rotating components are contained inside a pressure vessel.

Revision 2 of this report is issued to incorporate changes to the flywheel design. As a result of progress in the detailed design efforts and an increase in the required inertia, there have been significant changes to the high-inertia flywheel design. The flywheel changes include both configuration changes and a change from depleted uranium to tungsten heavy alloy as the high density flywheel material.

The pump design includes flywheel assemblies in two locations to provide the inertia required for pump coastdown. Each flywheel assembly consists of a cylindrically shaped set of heavy metal inserts held against a Type 403 stainless steel inner hub by an 18Ni maraging steel outer retainer cylinder and hermetically sealed on the ends by nickel-chromium-iron alloy (Alloy 690) plates and on the outside diameter by a thin shell of nickel-chromium-iron alloy (Alloy 690). Flywheel evaluations have been completed to determine the component shrink-fit requirements, the outer retainer cylinder primary stress, and the outer retainer cylinder critical flaw sizes. Also, missile penetration calculations were performed to evaluate the capacity of the pressure boundary structures to absorb the energy of the heavy metal inserts in the unlikely event of a flywheel fracture.

The flywheel structure was evaluated to ensure calculated stresses of all structural components (inner hub, heavy metal inserts, and outer retainer cylinder) are less than the applicable stress limits at assembly and all operating conditions.

The calculated stresses in the outer retainer cylinder during both normal operating conditions (1800 rpm) and design conditions (2250 rpm) are less than the applicable stress limits.

Results of a fracture mechanics evaluation show that the critical flaw size is well within ultrasonic inspection technique capability.

Missile penetration calculations show that in the unlikely event of a flywheel fracture, the flywheel heavy metal inserts will not have sufficient energy to penetrate the pump pressure boundary structures.

1.0 INTRODUCTION

This report summarizes the evaluation of the revised design of the high inertia flywheel assembly for the AP1000 reactor coolant pump. The geometry analyzed is based on the overall lengths and diameters derived from the pump outline drawing (Reference 1). The flywheel assembly design consists of a cylindrically shaped set of heavy metal inserts held against a Type 403 stainless steel inner hub by an 18Ni maraging steel outer retainer cylinder and hermetically sealed on the ends by nickel-chromium-iron alloy (Alloy 690) plates and on the outside diameter by a thin shell of nickel-chromium-iron alloy (Alloy 690). Radial shrink fits are imposed at assembly to prevent slippage between the shaft, the inner hub, the heavy metal inserts, and the outer retainer cylinder during pump operation. This study derives and compares stress values consistent with the non-local primary stresses reported for the depleted uranium flywheel for the AP600 evaluation (Reference 2) and the previous AP1000 evaluation in Revision 1 of this report.

The reactor coolant pump in the AP1000 design is a single-stage, hermetically sealed, high-inertia, centrifugal canned-motor pump. A canned-motor pump contains the motor and all rotating components inside a pressure vessel. The reactor coolant pump design is illustrated in Figure 3-1.

The reactor coolant pump pressure boundary shields the balance of the reactor coolant pressure boundary from theoretical worst-case flywheel failures. The reactor coolant pump pressure boundary (stator shell, flange, and casing) is analyzed to demonstrate that a fractured flywheel cannot breach the reactor coolant pump pressure boundary and impair the operation of safety-related systems and components. This meets the requirements of General Design Criteria 4. The reactor coolant pump flywheel is designed, manufactured, and inspected to minimize the potential for the generation of high-energy fragments (missiles) under any anticipated operating or accident condition consistent with the intent of the guidelines set forth in Standard Review Plan Section 5.4.1.1 and Regulatory Guide 1.14. Each flywheel is tested at an overspeed condition to verify the flywheel design and construction.

2.0 SUMMARY OF RESULTS

The calculations and evaluations contained in this report show that the results of the AP1000 flywheel stress and missile containment studies are comparable to those of the AP600 and those of the AP1000 analyses contained in Revision 1 of this report.

The applicable stress limits are derived from the American Society of Mechanical Engineers (ASME) Boiler and Pressure Vessel Code, Section III (Reference 4); the Standard Review Plan, NUREG-0800 Section 5.4.1.1 (Reference 5); and Regulatory Guide 1.14 (Reference 6). Both normal operating conditions (1800 rpm) and design conditions (125% overspeed = 2250 rpm) were evaluated. The following summarizes the results of the evaluation.

- A total radial shrink fit of 0.060 inches was calculated for assembly of the outer retainer cylinder, which ensures maintenance of the shrink fit during all operating conditions.
- The calculated primary stresses in the outer retainer cylinder, due to pump rotation for both normal and design conditions, are less than the allowable stress limits for the respective operating condition.
- The fracture mechanics evaluation of the outer retainer cylinder indicates that for assembly plus design conditions, the critical flaw size was a corner flaw having a depth of 0.265 inches and surface length of 0.795 inches. This size is compatible with ultrasonic inspection capabilities.
- The flywheel heavy metal inserts that contain the maximum kinetic energy were shown to not have sufficient energy to penetrate the adjacent pressure boundary components.

The details of the evaluations are provided in section 5.

3.0 DESCRIPTION OF COMPONENTS

The reactor coolant pump in the AP1000 design is a single-stage, hermetically sealed, high-inertia, centrifugal canned-motor pump. A canned-motor pump contains the motor and all rotating components inside a pressure vessel. The pressure vessel consists of the pump casing, stator closure, stator main flange, stator shell, stator lower flange, and stator cap, which are designed for full reactor coolant system pressure. Two flywheel assemblies provide the required pump coastdown time. The larger of the two flywheel assemblies is located between the motor and pump impeller. This flywheel assembly is protected from direct exposure to the hot primary water by the thermal barrier/stator closure. The smaller assembly is located within the canned motor at the thrust bearing, between the upper and lower thrust runner.

Surrounding the larger flywheel assembly are the heavy walls of the casing, thermal barrier, and stator closure, and surrounding the smaller flywheel assembly is the heavy wall of the stator lower flange. The reactor coolant pump concept is shown in Figure 3-1.

The flywheel assembly design consists of a cylindrically shaped set of heavy metal inserts held against a Type 403 stainless steel inner hub by an 18Ni maraging steel outer retainer cylinder and hermetically sealed on the ends by nickel-chromium-iron alloy (Alloy 690) plates and on the outside by a thin shell of nickel-chromium-iron alloy (Alloy 690). Radial shrink fits are used at assembly to prevent slippage due to motor torque between the shaft, the inner hub, the heavy metal inserts, and the outer retainer cylinder during pump operation. The outer retainer cylinder has the same axial length as the heavy metal inserts while the inner hub and thin outer shell are axially longer to provide weld joints for securing and hermetically sealing the end plates to the inner hub and the outer thin shell.

AP1000 RCP
PRELIMINARY
SEPT 15, 2006

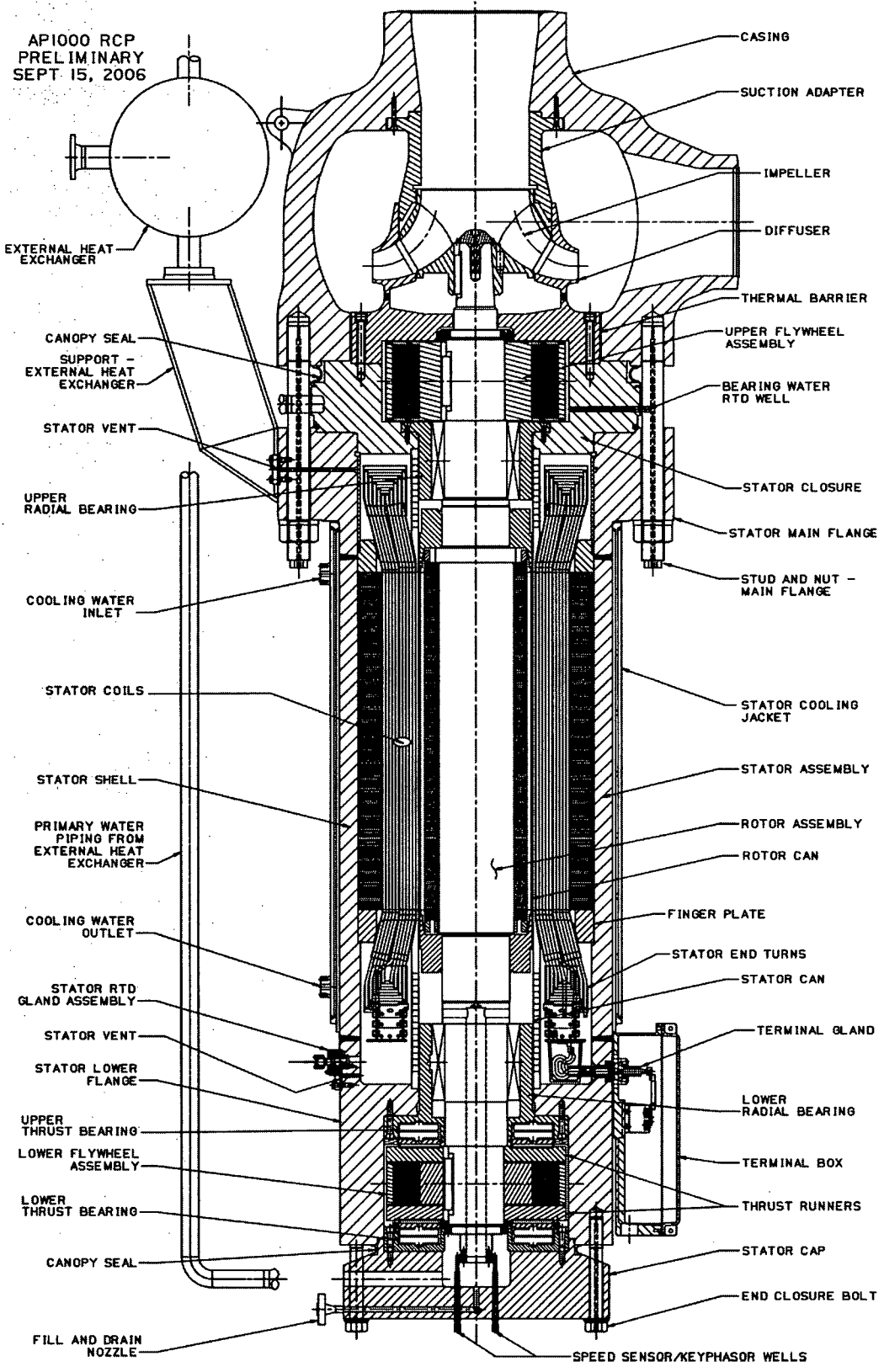


Figure 3-1 AP1000 Canned-Motor Reactor Coolant Pump

4.0 DESIGN REQUIREMENTS

The design requirements for the flywheel are based on the AP1000 RCP Design Specification (Reference 7) and the requirements outlined in the AP1000 Design Control Document (DCD) (Reference 3).

4.1 LOADING CONDITIONS

The loading conditions applicable to the flywheel are summarized below:

- Design Pressure 2500 psia
- Design Temperature 650°F for primary coolant water
550°F estimated maximum for upper flywheel
300°F estimated maximum for lower flywheel
- Design Speed 2250 rpm
- Operating Pressure 2250 psia
- Operating Temperature 537.2°F for primary coolant water
400°F estimated maximum for upper flywheel
200°F estimated maximum for lower flywheel
- Normal Operating Speed 1800 rpm
- Transients The flywheels operate in the bearing water environment that is thermally isolated from the primary coolant by the reactor coolant pump thermal barrier. With the exception of the startup and shutdown transients, it is assumed that the primary coolant transients will have a negligible affect on the flywheel. The design specification requires that 3,000 startup/shutdown cycles will be considered.
- Design Mechanical Loads The AP1000 reactor coolant pump motor synchronous speed is 1800 rpm. It is required that the pump be capable of speeds up to 1.25 times the normal operating speed or 2250 rpm. There is an external applied force on the flywheel assembly enclosure due to the pump internal pressure. In

addition, there are loads associated with the shrink fits between the flywheel and the shaft, and between the outer retainer ring and the heavy metal inserts and inner flywheel hub.

4.2 CRITERIA

The design criteria for the flywheel assembly are given in the AP1000 RCP Design Specification (Reference 7) and are outlined in subsection 5.4.1 of the AP10000 DCD (Reference 3). The applicable stress limits are derived from the ASME Code, Section III (Reference 4), Standard Review Plan, subsection 5.4.1.1 (Reference 5), and Regulatory Guide 1.14 (Reference 6). These limits are addressed in the following subsections.

In addition to the previous criteria, the flywheel complies with the requirement of GDC 4, which requires that components important to safety be protected against the effects of missiles. It is demonstrated in section 5.2 that in the event of a potential worst-case failure, the energy of the flywheel heavy metal inserts is contained by the casing, thermal barrier, stator closure, and stator lower flange.

4.2.1 American Society of Mechanical Engineers Code

The Level A stress limits of the ASME Code, Section III, Subsection NG (Reference 4) are used as evaluation criteria for the components of the flywheel assembly. Subsection NG rules and limits apply to reactor core support structures. The use of core support limits is considered appropriate for the flywheel assembly components since both the core supports and flywheel assembly operate in the reactor water environment and neither is a reactor coolant pressure boundary. An additional acceptance criterion is a limit of S_y for the primary plus secondary membrane plus bending stress intensities in the main shrink-fit areas. This ensures that the flywheel will remain elastic in these areas and prevent a loss of shrink fit due to yielding.

4.2.2 Regulatory Guide 1.14

The application of the guidance of Regulatory Guide 1.14 for the analysis of the flywheel is addressed in the AP1000 DCD (Reference 3). As outlined in the DCD, the flywheel assembly is evaluated for three critical flywheel failure modes. This report demonstrates that the failure modes of ductile fracture, non-ductile fracture, and excessive deformation will not occur at the

design speed (125-percent normal speed). The design speed envelopes all expected and postulated overspeed conditions, including overspeeds due to postulated pipe ruptures.

The analysis performed to evaluate the failure by ductile fracture uses the faulted stress limits in Appendix F of Section III of the ASME Code as acceptance criteria.

The enclosure is evaluated at normal operating and design speeds using the ASME Code, Section III, Subsection NG limits. The enclosure components of the flywheel assembly (Alloy 690 end plates and thin outer shell) are not evaluated for critical failure speed. The function of the enclosure is to prevent contact of reactor coolant with the heavy metal inserts and outer retainer cylinder of the flywheel assembly. No credit is taken in the evaluation of missiles from a postulated flywheel fracture for the containment of fragments by the enclosure components. In addition, the enclosure components contribute only a small portion of the total energy in the rotating assembly.

The analysis performed to evaluate the potential for nonductile fracture of the outer retainer cylinder (18Ni maraging steel) considers the estimate of the flaw size, location, and values of fracture toughness assumed for the material. An evaluation of nonductile fracture for the outer retainer cylinder, summarized in section 5.1, determines critical flaw size.

Failure by excessive deformation is defined as any deformation, such as enlargement of the bore, which could cause separation directly or could cause an unbalance of the flywheel. The evaluation of excessive deformation verifies that the components of the flywheel assembly remain in contact at the design speed.

4.2.3 Standard Review Plan

The heavy metal alloy flywheel is evaluated using the stress limits given in paragraphs 4.a and 4.c of the Standard Review Plan, subsection 5.4.1.1 (Reference 5) for normal and design speed. Paragraph 4.a recommends that at normal operating speed, the combined stresses due to centrifugal forces and interference fits should not exceed 1/3 of the minimum yield strength. Paragraph 4.c recommends that at design overspeed (125 percent of normal speed), the combined stresses due to centrifugal forces and interference fit should not exceed 2/3 of the minimum specified yield strength. These limits are satisfied for the outer retainer cylinder. The Standard Review Plan limits do not apply to the enclosure components.

5.0 ANALYTICAL METHODS AND RESULTS

This section describes the components involved in the analysis, the methods of analyses for the studies, and the results.

The flywheel scoping calculations focus on determining the component shrink-fit requirements, the outer retainer cylinder primary stress, and the outer retainer cylinder critical flaw size. The AP1000 flywheel location within the thermal barrier/stator closure is similar to the AP600 design. The AP1000 has a second, shorter flywheel located within the canned motor between the thrust runners within the stator lower flange. In both locations, the basic design concept of the flywheels has been changed to replace the shrunk-fit depleted uranium disks considered in the AP600 design with tungsten heavy metal alloy segments that are held against a Type 403 stainless steel inner hub by an 18Ni maraging steel outer retainer cylinder. The AP1000 flywheel has the same primary stress limits as those defined for the AP600. The heavy metal alloy and outer retainer cylinder are sealed from the reactor coolant by an enclosure (inner hub, end plates, and outer thin shell) that also must satisfy the stress requirements of Subsection NG of the ASME Code, Section III.

The missile penetration calculations evaluate the capacity of the pressure boundary structures to absorb the energy of the heavy metal inserts. The missiles are not to penetrate the pressure boundary wall, so containment is preserved. This AP1000 study uses the same missile containment calculation procedure as AP600.

5.1 FLYWHEEL CALCULATIONS

The flywheel primary stress analyses are performed by hand calculations assuming that the assembly consists of a cylindrically shaped set of heavy metal inserts held against a Type 403 stainless steel inner hub by an 18Ni maraging steel outer retainer cylinder in an enclosure and shrunk onto the shaft (Figures 5-1 and 3-1). Using simplified methods, normal operating speed (1800 rpm) at steady-state operating temperature (400°F) and design overspeed (2250 rpm) at steady-state design temperature (550°F) of the motor cavity flywheel are investigated. The analyses conservatively neglect the effects of system pressure. The results of these analyses are summarized as follows:

- The calculated primary stresses in the outer retainer cylinder due to pump rotation are:
 - 56.6 ksi for normal speed (1800 rpm)
 - 88.4 ksi for design speed (2250 rpm)

These calculated stresses are less than the allowable stress limits for 18Ni maraging steel (AMS 6519B).

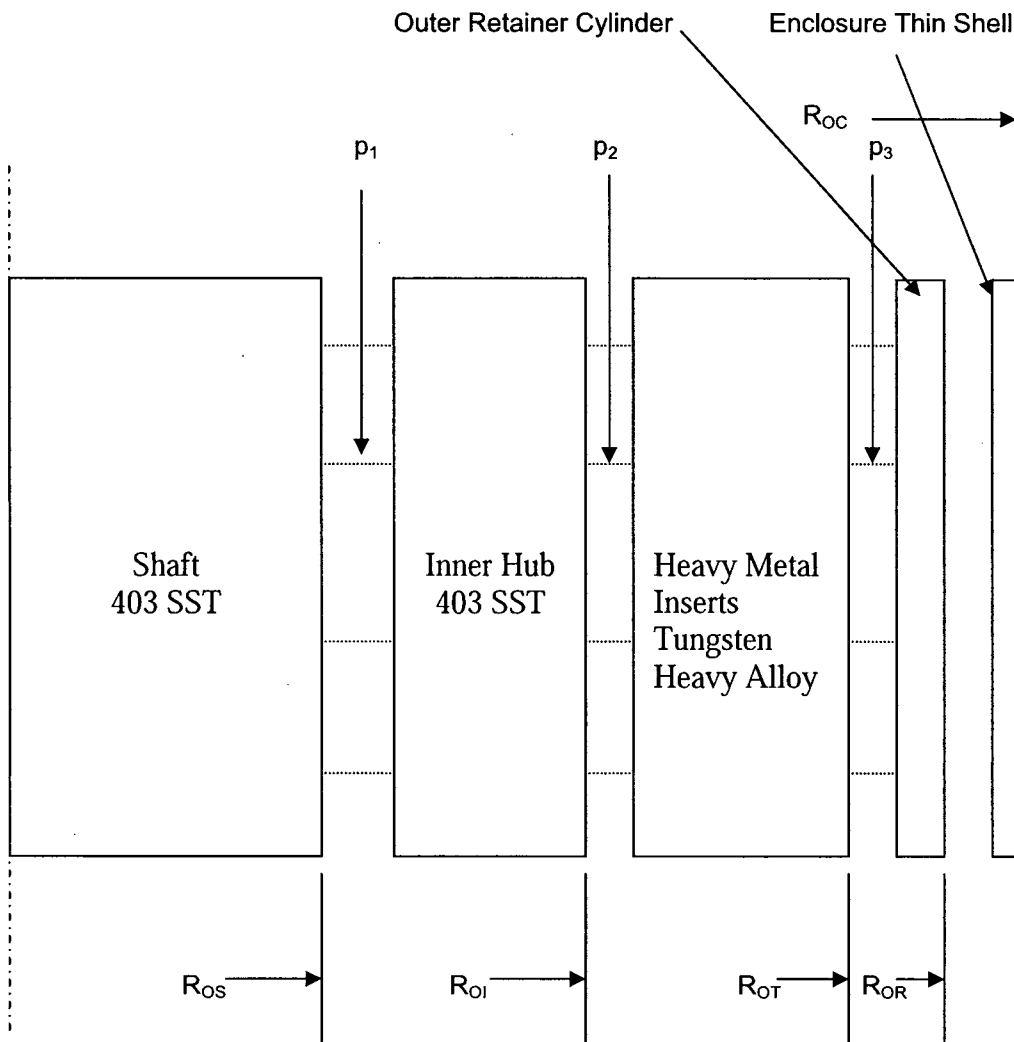
- Based on a material yield stress of 233.6 ksi at 400°F, the normal condition primary stress limit is $S_y/3 = 77.9$ ksi.
 - Based on a material yield stress of 225.6 ksi at 550°F the design condition primary stress limit is $2S_y/3 = 150.4$ ksi.
- A preliminary fracture mechanics evaluation of the AP1000 outer retainer cylinder for sudden rupture indicates that for the maximum hoop stress at the cylinder inside surface, which occurs for assembly plus 125-percent overspeed, the critical flaw size is 0.265 inches deep with a surface length of 0.795 inches. This flaw size compares favorably with ultrasonic inspection capability.

5.1.1 Analytical Model

The calculations for the AP1000 motor cavity flywheel assembly are performed via hand calculations considering a series of concentric rings shrunk fit together to make the assembly. These rings and pertinent geometrical properties for both flywheels are illustrated in Figure 5-1. The only difference in the two flywheels is the length, which is 15.50 inches for the larger flywheel and 8.50 inches for the smaller flywheel. The enclosure thin shell is illustrated and serves as a sealing membrane but does not contribute structurally. For the present analysis, the material for the rotor shaft and inner hub are 403 stainless steel (ASTM A336, Grade F6), the heavy metal alloy segments are tungsten heavy alloy (ASTM B777, Class 4), the outer retainer cylinder is 18Ni maraging steel (AMS 6519, Vascomax® T250), and the enclosure components (end plates and outer thin shell) are nickel-chromium-iron alloy (Alloy 690, ASTM B564, UNS N06690). The outer retainer cylinder ring is conservatively evaluated for shaft rotations at 1800 and 2250 rpm and steady-state temperatures of 400°F and 550°F respectively while conservatively neglecting the effects of system pressure.

The mechanical properties for the flywheel are presented in Table 5-1. The properties for Type 403 stainless steel are taken from ASTM A336, Grade F6 with modified chemistry and property requirements, the Tungsten Heavy Alloy properties are from ASTM B777 and the 18Ni maraging properties are from AMS 6519 and Reference 12. The properties for Alloy 690 are taken from the ASME Code.

Table 5-1 Mechanical Properties			
Component	Yield Strength (ksi)	Mean Expansion Coefficient (in./in.-°F)	Density (lb/in³)
Shaft and Inner Hub (Type 403 stainless steel)	40	6.2×10^{-6}	0.280
Tungsten Heavy Alloy	75	2.5×10^{-6}	$\rho_T = 0.67$
Outer Retainer Cylinder (18Ni maraging steel)	250 @ 70°F	6.13×10^{-6}	$\rho_R = 0.289$
	233.6 @ 400°F		
	225.6 @ 550°F		
End Plates and Thin Shell (Alloy 690)	35	7.9×10^{-6}	0.293



- p_1 = the interface pressure between the shaft and the inner hub
- p_2 = the interface pressure between the inner hub and the heavy metal inserts
- p_3 = the interface pressure between the heavy metal inserts and the outer retainer cylinder
- R_{OS} = the shaft outer radius and the inner hub inner radius = []^{a,b} inches
- R_{OI} = the inner hub outer radius and the heavy metal inner radius = []^{a,b} inches
- R_{OT} = the heavy metal outer radius and the retainer cylinder inner radius = []^{a,b} inches
- R_{OR} = the retainer cylinder outer radius and the can inner radius = []^{a,b} inches
- R_{OC} = the enclosure can outer radius = []^{a,b} inches

Figure 5-1 Flywheel Assembly Dimensions

5.1.2 Concentric Ring Model Geometry and Shrink-Fit

The flywheel assembly will be manufactured by shrink fitting the outer retainer cylinder onto the outside diameter of the heavy metal inserts, which have been fitted to the outside diameter of the inner hub, with []^{a,b} inches of radial interference. Enclosure completion, for the purpose of sealing the heavy metal alloy inserts and 18Ni maraging steel outer retainer cylinder from the reactor coolant, is accomplished by assembling and welding end plates (Alloy 690) to the inner hub and then assembling and welding the outer thin shell (Alloy 690) to the end plates. The shaft fit bore of the flywheel inner hub is machined to final size after completing the flywheel fabrication to achieve a []^{a,b} inch radial interference on the rotor shaft.

To preclude possible slippage between components that could change the balance of the flywheel, the shrink fit and outer retainer cylinder thickness are sized to maintain a shrink fit at all possible conditions. In addition to the shrink fit, the heavy metal inserts are keyed to the inner hub axially at mid-height and circumferentially at the intersection of each heavy metal insert with keys designed to carry the maximum torque of the motor and seismic loads. The total radial interference of []^{a,b} inches in the assembly of the flywheel was selected to maintain an interference fit at the heavy metal insert to inner hub interface under the worst case with the flywheel at 125-percent overspeed and ambient conditions (zero external pressure and 70°F). Unlike the uranium insert flywheel design, the enclosure components (end plates and outer thin shell) have a negligible impact on the shrink fit of the outer retainer cylinder on the heavy metal inserts and inner hub and are not relied upon structurally.

5.1.3 Outer Retainer Cylinder Rotational Primary Stresses

Per the AP1000 RCP Design Specification (Reference 7), the design speed of the flywheel is defined as 125% of the normal speed of the motor. At normal speed the calculated maximum primary stresses in the outer retainer cylinder shall be limited to less than 1/3Sy. At the design speed the calculated maximum primary stress in the outer retainer cylinder shall be limited to less than 2/3Sy. The calculations for these primary stresses due to rotation consider only the heavy metal alloy and outer retainer cylinder portion of the flywheel assembly and do not include any of the stresses due to component shrink fits or the shrink fit of the flywheel assembly onto the shaft.

The maximum primary stress in the outer retainer cylinder, due to the centrifugal forces of the heavy metal inserts and the outer retainer cylinder inertia, is the hoop stress at the inner radius of the outer retainer cylinder. The calculations for the hoop stress are given as follows:

- Outer retainer cylinder inner radius hoop stress due to centrifugal acceleration of heavy metal inserts and the outer retainer cylinder

$$\sigma_{\theta\theta}(R_{OT})_R = (\sigma_{\theta P} + \sigma_{\theta\omega})$$

- Hoop stress in outer retainer cylinder due to centrifugal acceleration of heavy metal inserts

$$\sigma_{\theta P} = \frac{P_{OT} R_{OT}}{(R_{OR} - R_{OT})}$$

- Pressure exerted by heavy metal inserts on the outer retainer cylinder

$$P_{OT} = \frac{\rho_T G_\omega (R_{OT}^2 - R_{OI}^2)}{2R_{OT}}$$

- Centrifugal acceleration of heavy metal inserts

$$G_\omega = \frac{\omega^2}{g} \cdot \frac{2\sin(\alpha)}{3\alpha} \cdot \left(R_{OT} + R_{OI} - \frac{R_{OT} \cdot R_{OI}}{R_{OT} + R_{OI}} \right)$$

Where $g = 386.4 \text{ in/sec}^2$

- Outer retainer cylinder inner radius hoop stress due to centrifugal acceleration of outer retainer cylinder.

$$\sigma_{\theta\omega} = \frac{\rho_R \omega^2}{4g} [(3 + \nu) R_{OR}^2 + (1 - \nu) R_{OT}^2]$$

Where ν (Poisson's ratio) is conservatively assumed as 0.3

Outer retainer cylinder normal operation inner radius hoop stress

$$\sigma_{\theta\theta}(R_{OT})_R = (47,993 \text{ psi} + 8,555 \text{ psi}) = 56,548 \text{ psi}$$

$$\sigma_{\theta P} = \frac{3,928 \text{ psi} \times []^{a,b} \text{ in}}{([]^{a,b} \text{ in} - []^{a,b} \text{ in})} = 47,993 \text{ psi}$$

$$P_{OT} = \frac{0.67 \frac{\text{lb}}{\text{in}^3} \cdot 1,298.5 \cdot (([]^{a,b} \text{ in})^2 - ([]^{a,b} \text{ in})^2)}{2 \cdot ([]^{a,b} \text{ in})} = 3,928 \text{ psi}$$

$$G_{\omega} = \frac{\left(188.5 \frac{\text{rad}}{\text{sec}}\right)^2}{386.4 \frac{\text{in}}{\text{sec}^2}} \cdot \frac{2 \sin(0.2618 \text{ rad})}{3 \cdot 0.2618 \text{ rad}} \cdot \left([]^{a,b} \text{ in} + []^{a,b} \text{ in} - \frac{[]^{a,b} \text{ in} \cdot []^{a,b} \text{ in}}{[]^{a,b} \text{ in} + []^{a,b} \text{ in}} \right) = 1,298.5$$

$$\sigma_{\theta\omega} = \frac{0.289 \frac{\text{lb}}{\text{in}^3} \left(188.5 \frac{\text{rad}}{\text{sec}}\right)^2}{4 \times 386.4 \frac{\text{in}}{\text{sec}^2}} [(3 + 0.3)([]^{a,b} \text{ in})^2 + (1 - 0.3)([]^{a,b} \text{ in})^2] = 8,555 \text{ psi}$$

Outer retainer cylinder design condition inner radius hoop stress

$$\sigma_{\theta\theta}(R_{OT})_R = (74,995 \text{ psi} + 13,367 \text{ psi}) = 88,362 \text{ psi}$$

$$\sigma_{\theta P} = \frac{6,138 \text{ psi} \times []^{a,b} \text{ in}}{([]^{a,b} \text{ in} - []^{a,b} \text{ in})} = 74,995 \text{ psi}$$

$$P_{OT} = \frac{0.67 \frac{\text{lb}}{\text{in}^3} \cdot 2,028.9 \cdot (([]^{a,b} \text{ in})^2 - ([]^{a,b} \text{ in})^2)}{2 \cdot ([]^{a,b} \text{ in})} = 6,138 \text{ psi}$$

$$G_{\omega} = \frac{\left(1.25 \cdot 188.5 \frac{\text{rad}}{\text{sec}}\right)^2}{386.4 \frac{\text{in}}{\text{sec}^2}} \cdot \frac{2 \sin(0.2618 \text{ rad})}{3 \cdot 0.2618 \text{ rad}} \cdot \left([]^{a,b} \text{ in} + []^{a,b} \text{ in} - \frac{[]^{a,b} \text{ in} \cdot []^{a,b} \text{ in}}{[]^{a,b} \text{ in} + []^{a,b} \text{ in}} \right) = 2,028.9$$

$$\sigma_{\theta\omega} = \frac{0.289 \frac{\text{lb}}{\text{in}^3} \left(1.25 \cdot 188.5 \frac{\text{rad}}{\text{sec}}\right)^2}{4 \times 386.4 \frac{\text{in}}{\text{sec}^2}} [(3 + 0.3)([]^{a,b} \text{ in})^2 + (1 - 0.3)([]^{a,b} \text{ in})^2] = 13,367 \text{ psi}$$

The outer retainer cylinder is 18Ni maraging steel, and the yield stress for this material is 233,600 psi at 400°F and 225,600 psi at 550°F. Per the design specification, the 1/3Sy is 77,900 psi at 400°F and 2/3Sy is 150,400 psi at 550°F. For normal operation at a rotational speed of 1800 rpm and a steady-state temperature of 400°F, the maximum primary hoop stress is 56,548 psi, which is less than 77,900 psi. Additionally, for a design rotational speed of 2250 rpm and a steady-state temperature of 550°F, the maximum primary hoop stress is 88,362 psi, which is less than 150,400 psi. Since the maximum primary stresses due to rotation for the outer retainer cylinder are less than the prescribed allowable stresses, the requirements of the design specification are satisfied.

5.1.4 Concentric Ring Elastic Hoop Stresses

In Table 5-2, the hoop stresses at the inner and outer diameter of each of the concentric rings in the model are presented for assembly conditions and 125-percent overspeed at 70°F. From Table 5-2, it is noted that the maximum compressive stresses of 29.6 ksi in the inner hub and 32.7 ksi in the shaft are less than the yield stress for Type 403 stainless steel, which is 40 ksi at 70°F. In addition, the maximum hoop stresses of 98.5 ksi at the inner radius of the outer retainer cylinder is less than the yield stress for 18Ni maraging steel, which is 250 ksi at 70°F.

Table 5-2 AP1000 Motor Cavity Flywheel Hoop Stresses					
	Shaft	Inner Hub		Outer Retainer Cylinder	
	Outer Radius S_{USO} (psi)	Inner Radius S_{UII} (psi)	Outer Radius S_{UIO} (psi)	Inner Radius S_{URI} (psi)	Outer Radius S_{URO} (psi)
Assembly ⁽¹⁾	- 32,777	- 29,629	- 12,445	87,650	79,519
125-Percent Overspeed at 70°F	229	5,822	2,549	98,537	89,405

1. Assembly radial shrink fits:
 Flywheel assembly to rotor shaft = []^{a,b} inches
 Outer retainer cylinder to Heavy Metal Alloy = []^{a,b} inches

5.1.5 Flywheel Enclosure Welds

Since the flywheel enclosure is not considered to be a “reactor coolant pressure boundary,” the stress analysis of the enclosure welds has been deferred until the detailed final design of the flywheel is complete. However, with the change in flywheel design, the magnitude of displacements the enclosure components and welds (end plates and outer can) are subjected to during operation have been reduced an order of magnitude when compared to the uranium insert design. Therefore, it is expected that the AP1000 flywheel enclosure component and weld stresses will meet the ASME Code limits during operation at both normal and design speeds including thermal transients.

5.1.6 Fracture Mechanics of Outer Retainer Cylinder

An estimate of the critical flaw size in the outer retainer cylinder of the flywheel was made using fracture mechanics technology. The most limiting situation for fracture is for a flaw emanating from the inside surface of the cylinder and subjected to the stresses at the 125% speed condition. This flaw is assumed to be in the radial-axial plane and thus perpendicular to the hoop stress direction, which is the most severe orientation. Further, the flaw is conservatively assumed to have a semi-elliptical shape with a surface length to depth ratio of 6:1, as in Section XI of the ASME Code, when remote from the cylinder ends. In the present analysis, the flaw is also assumed to be at the most detrimental position along the length of the cylinder, where it becomes a corner flaw with a surface length to depth (length along the other cylinder surface) ratio of 3:1. The hoop stress at the 125% speed condition at the cylinder inside surface is 98,537 psi. This stress was assumed to be uniform across the cylinder wall. Values of K_I (mode I plane strain stress intensity factor) were computed as a function of crack depth with the NASCRAC fracture mechanics software (NASA Crack Analysis Code, Version 3, Failure Analysis Associates, Menlo Park, California). The room temperature fracture toughness (K_{IC}) of the T250 18Ni maraging steel material was taken as 89,000 psi-in^{1/2}, the minimum value in Reference 12. The critical flaw size was for a corner flaw having a depth of 0.265 inches and surface length of 0.795 inches. A flaw of this size is detectable with ultrasonic inspection techniques and can be used to support fracture toughness and inspection requirements for the T250 18Ni maraging outer retainer cylinder.

5.2 MISSILE PENETRATION

This analysis (reference 11) follows the same procedure used for turbine disk fractures in Reference 10 and previous analysis (references 8 and 9) for the depleted uranium flywheel. Although no significant flaws are expected in the maraging steel outer cylinder of the flywheels that completely contain the twelve (12) heavy metal blocks, this analysis assumed a fracture of the maraging steel outer cylinder has occurred and shows that the energy of the fragments is insufficient to penetrate the pressure boundary. No other effects of a flywheel failure were considered in this evaluation.

5.2.1 Assumptions

The method of analysis of Reference 10, which was developed from scale tests of turbine disks, is considered applicable herein with the following conservative assumptions used.

- The outer maraging steel retainer cylinder and outer thin shell of the flywheel were neglected. In reality the outer retainer cylinder and outer thin shell would need to be breached in the unlikely event of an outer retainer cylinder fracture before the pressure boundary being impacted by the heavy metal alloy. This analysis completely ignored the maraging steel outer retainer cylinder and outer thin shell components.
- The Alloy 690 end plates/welds and the surrounding water were also neglected from the energy absorption calculations.
- The minimum ASME material strength properties at temperature were used for the pressure boundary (containment closure). The pressure boundary material is taken to be CF8 or F304 SS at a design temperature conservatively estimated to be 550°F.
- All heavy metal segments were considered to impact the pressure boundary.
- No secondary effects of the shrink fit of the flywheel assembly were considered.
- The shell containment in line with the flywheel heavy metal segments was the only containment material considered.
- The design speed of 125 percent times the operating speed of 1800 rpm was used.

5.2.2 Energy Analysis

The containment of disk fragments by a cylinder shell is a two-stage process, per Reference 10. The first stage involves inelastic impact and transfer of momentum to the containment cylinder. If the energy dissipated in plastic compression and shear strain is sufficient to accommodate the loss of kinetic energy of the flywheel, there is no shear perforation of the shell. The process then enters Stage 2, which involves dissipation of energy in plastic tensile strain in the shell. For containment, the energy dissipated in plastic tensile strain must accommodate the residual kinetic energy of the flywheel. Note the procedure has experimental verification of the analytical techniques (Reference 10). The kinetic energy of a fragment is:

$$\frac{1}{2}MV^2, \text{ where } M = \text{mass of fragment and } V = \text{fragment velocity after rupture}$$

Fragment rotational considerations can be neglected per Reference 10. The flywheel heavy metal alloy is assembled into a cylindrical ring using individual wedge shaped segments arranged in keystone fashion and retained against the inner hub by the outer retainer cylinder. Therefore, in the unlikely event of a fracture in the outer retainer cylinder of the flywheel assembly, it has been conservatively assumed that all individual heavy metal alloy segments simultaneously strike the pressure boundary.

Two cases of the containment shell model are considered. Case A, for the upper flywheel, is conservatively assumed to be through the thermal barrier material and the adjacent stator closure. Case B, for the lower flywheel, is through the stator lower flange. The analysis model gives the containment thickness of the two cases in Table 5-3.

Case	Inner Radius	Outer Radius	Thickness
A – Upper (larger) Flywheel	18.97"	25.25"	6.28"
B – Lower (smaller) Flywheel	18.75"	27.69"	8.94"

5.2.3 Missile Containment Analysis Results

The pressure boundary sections contain the kinetic energy of all heavy metal alloy segments simultaneously. The verified semi-empirical method of Reference 10 shows that any improbable flywheel fracture would not penetrate the thermal barrier/stator closure walls that surround the upper larger flywheel assembly nor the stator lower flange closure walls that surround the smaller lower flywheel.

The following Table 5-4 compares the heavy metal energy to the energy available for the Stage 1 (shear) penetration and for the Stage 2 (tensile) penetration. The ratio of the two gives the third column of results that is presented as margin.

5.2.4 Conclusion

The analysis shows that even in the unlikely event of the flywheel failure, any loose parts (missiles) will be contained within the primary pressure boundary.

Table 5-4 Pressure Boundary Capacity for Missile Containment			
Case	Fragment Energy (in-lb)	Energy Required for Penetration (Boundary Capacity) (in-lb)	Margin
Case A -- Stage 1	36,340,000	247,940,000	6.8
- Stage 2	54,410,000	100,070,000	1.8
- Total	90,750,000	348,010,000	3.8
Case B -- Stage 1	28,870,000	392,780,000	15.1
- Stage 2	20,890,000	85,640,000	4.1
- Total	49,760,000	478,420,000	9.6

6.0 REFERENCES

1. APP-MP01-V2-001 thru 002, Rev. 1 and APP-MP01-V2-003 thru 008, Rev. 0, "AP1000 Reactor Coolant Pump - Outline."
2. WCAP-13734, "Structural Analysis Summary for the AP600 Reactor Coolant Pump High Inertia Flywheel." May 1993.
3. APP-GW-GL-700, Revision 15, "AP1000 Design Control Document," subsection 5.4.1.
4. ASME Boiler and Pressure Vessel Code, Section III, Subsection NG and Appendices, 1998 Edition, American Society of Mechanical Engineers, New York, N.Y.
5. NUREG-0800, "Standard Review Plan," Revision 1, Section 5.4.1.1, U.S. Nuclear Regulatory Commission, Office of Nuclear Regulation, Washington, D.C., July 1981.
6. Regulatory Guide 1.14, Revision 1, "Reactor Coolant Pump Flywheel Integrity," U.S. Nuclear Regulatory Commission, Office of Standard Development, Washington, D.C., August 1975.
7. APP-MP01-M2-001, Rev. C, "AP1000 RCP Design Specification"
8. Dietrich, D. E., "AP1000 RCP Concept Design Flywheel Scoping, Missile Containment, and Rotor Critical Speed Calculations," Westinghouse Government Services Company LLC, Electro-Mechanical Division, Analytical Technologies Letter AT/S-02-17, Revision 1, May 21, 2002.
9. Brose, W. R. and Dietrich, D. E., "Updated Analysis of Missile Containment for AP1000 RCP Concept Design Flywheel," Curtiss-Wright Electro-Mechanical Corporation, Analytical Technologies Letter AT/S-02-40, November 21, 2002.
10. Hagg, A. C., and Sankey, G. O., "The Containment of Disk Burst Fragments by Cylindrical Shells," ASME Paper 73-WA-Pwr-2, 11/73; also in ASME Journal of Engineering for Power, 4/74, pg. 114-123.
11. Casamassa, J. and Brose, W. R., "Pressure Boundary Containment of a Burst Tungsten Flywheel", Curtiss-Wright Electro-Mechanical Corporation, Analytical Technologies Letter ET/S-06-31, Rev. 1, September 20, 2006.
12. "Vascomax Nickel Maraging Steels", Technical Data Sheet, Allvac, Allegheny Technologies, Monroe, North Carolina.

^a The information reveals the distinguishing aspects of a process or component, structure, tool, method, etc., and the prevention of its use by competitors of Curtiss-Wright Electro-Mechanical Corporation, without license from Curtiss-Wright Electro-Mechanical Corporation, gives Curtiss-Wright Electro-Mechanical Corporation a competitive economic advantage.

^b The information, if used by a competitor, would reduce the competitor's expenditure of resources or improve the competitor's advantage in the design, manufacture, shipment, installation, assurance of quality, or licensing of a similar product.